Journal of Power Sources 239 (2013) 24–29

Contents lists available at SciVerse ScienceDirect

Journal of Power Sources

journal homepage: www.elsevier.com/locate/jpowsour

Short communication

Porous $Co_{16}S_{16}O_{96}$ nanosheets as a new electrode material for use in supercapacitors

Lifeng Liu*

International Iberian Nanotechnology Laboratory (INL), 4715-330 Braga, Portugal

HIGHLIGHTS

- Facile synthesis of $Co_{16}S_{16}O_{96}$ nanosheets – a new electrode material.
- $Co_{16}S_{16}O_{96}$ nanosheets exhibit high specific capacitance and good rate capability.
- $Co_{16}S_{16}O_{96}$ nanosheets show a long cycling life with high capacity retention.

ARTICLE INFO

Article history:
Received 4 February 2013
Received in revised form
11 March 2013
Accepted 19 March 2013
Available online 30 March 2013

Keywords:
Electrode material
Hydrothermal synthesis
Nanosheet
Supercapacitor

ABSTRACT

Porous $Co_{16}S_{16}O_{96}$ (COD database code: 591-0314) nanosheets have been fabricated by a simple and low-cost hydrothermal approach. The as-fabricated $Co_{16}S_{16}O_{96}$ nanostructures are characterized by a porous interconnected sheet-like network and prove to be highly crystalline. Electrochemical tests reveal that the $Co_{16}S_{16}O_{96}$ nanosheets can be reversibly charged and discharged in a potential window between −0.05 and 0.4 V vs. saturated calomel electrode at various specific current densities ranging from 0.5 A g^{-1} to 50 A g^{-1}. The specific capacitance of these nanosheets is 333 F g^{-1} at 1 A g^{-1} in the beginning of cycling test, and increases with cycle numbers up to 386 F g^{-1}, then remaining constant till 4000 cycles. More remarkably, even at a current density as high as 50 A g^{-1}, the nanosheets still possess a specific capacitance of 170 F g^{-1}, and only lose 15.3% of the initial capacitance value after 4000 cycles, showing great promise for use as high-performance supercapacitor electrodes.

1. Introduction

As one of the most important types of energy storage devices, supercapacitors have received considerable attention in the past decade as they possess very high power density, satisfactory rate capability and excellent cycling performance, and therefore are believed to be a promising candidate that can bridge lithium-ion batteries and conventional dielectric capacitors for use in hybrid power sources [1].

Supercapacitors take advantage of either electrochemical double layers (ECDL) or pseudocapacitance arising from fast surface redox reactions to store electrical energy, for which three families of materials are commonly used, namely, carbon, conducting polymers and metal oxides. To date, a variety of nanostructures composed of these three families of materials have been extensively investigated [2–5], and specific capacitance as high as 2530 F g^{-1} measured at 0.61 A g^{-1} as well as excellent cycling performance up to 200,000 cycles have been recently achieved by manganese oxide films grown on carbon fiber paper [6]. Besides, metal hydroxides such as $Ni(OH)_2$ [7], $Co(OH)_2$ [8] and their composites [9] as well as metal sulfides like Co_xS_y [10–12] and CuS [13], also attracted great research interest in recent years and became a new class of candidate materials for supercapacitors. They have proved to have comparable or even much better electrochemical performance than metal oxides. For instance, it was observed that the nickel hydroxide directly electrodeposited on nickel foam current collector had unprecedentedly high specific capacitance of 3152 F g^{-1} at a charge/discharge current density of 4 A g^{-1} [7]; Lou and coworkers demonstrated that CoS_2 micro-ellipsoids and CuS nanoneedles can exhibit specific capacitance of 750 A g^{-1} at 5 A g^{-1} and 122 A g^{-1} at 1.2 A g^{-1}, respectively [12,13]. Although significant progress has been achieved so far, a continuing effort toward exploring new materials for use in supercapacitors is still very much in demand in that electrode material is one of the most important components of a supercapacitor, among others.

Herein, we report a new material exhibiting superior pseudocapacitive properties – $Co_{16}S_{16}O_{96}$ nanosheet, which was prepared by a simple and low-cost hydrothermal approach. We demonstrate

* Tel.: +351 253 140112; fax: +351 253 140119.
E-mail address: lifeng.liu@inl.int.

0378-7753/$ – see front matter © 2013 Elsevier B.V. All rights reserved.
http://dx.doi.org/10.1016/j.jpowsour.2013.03.109

that this unique material not only has high specific capacitance, but also reveals excellent cycling stability and very good rate capability.

2. Materials and methods

The $Co_{16}S_{16}O_{96}$ nanosheets were prepared as follows: 25 ml 0.01 M $Co(NO_3)_2 \cdot 6H_2O$ and 25 ml 0.01 M $Na_2S \cdot 9H_2O$ aqueous solutions were mixed dropwise into a beaker. Black precipitates immediately appeared upon blending, which are mainly composed of cobalt sulfide. The mixed solution was then transferred into a Teflon-lined stainless steel autoclave reactor. High-purity nitrogen (99.999%) was flowed into the reactor, resulting in an internal pressure of 6 bar. Subsequently, the reactor was heated at 180 °C for 18 h and then cooled down to room temperature. The internal pressure in the reactor was increased to 11 bar upon heating and maintained constant during the whole reaction process. The resulting black powders were collected by centrifugation, washed in de-ionized water and subjected to centrifugation once again. Afterward, the powders were dispersed into 0.5 ml de-ionized water to form slurry.

The morphology of the as-prepared nanostructures was characterized by scanning electron microscopy (SEM, FEI Quanta 650), and their crystallographic phase and microstructure were examined by X-ray diffractometry (XRD, Philips X'pert) using Cu $K\alpha$ irradiation ($\lambda = 1.5406$ Å) and transmission electron microscopy (TEM, FEI Titan ChemSTEM 80-200), respectively. The chemical state of the elements constituting the sample was checked by X-ray photoelectron spectroscopy (XPS, Thermo Scientific EscaLab 250Xi). The electrochemical tests were carried out in a three-electrode cell using a Pt wire as counter electrode and a saturated calomel electrode (SCE) as reference, respectively. The working electrode was prepared by spreading the slurry composed of the collected powders over a nickel foam current collector, followed by a thermal treatment in argon at 350 °C for 1 h. The mass of the active materials was around 1.1 mg, which was measured by a high-precision balance (Sartorius CPA225D) before slurry loading and after annealing. It was found that the black powders were able to strongly adhere to the surface of nickel foam after annealing, and did not fall off even if the nickel foam was mechanically bent. The cyclic voltammetry (CV) and galvanostatic charge/discharge test were performed in a 2 M KOH electrolyte using a multi-channel battery tester (Biologic VMP3). The electrode material was found to be chemically stable upon continuous cycling in the alkaline solution for at least one month. All chemicals used in the experiments were purchased from Sigma–Aldrich and of analytical grade.

3. Results and discussion

Fig. 1 shows representative SEM micrographs of the as-prepared nanostructures. It reveals that the sample has a feature size of several tens of nanometers. It is characterized by an interconnected network having an open porous structure. Upon closer examination, it is observed that the as-fabricated compound exhibits a sheet-like morphology, as displayed in Fig. 1b.

Fig. 2 represents a XRD pattern of the as-obtained nanosheets. The peaks at 24.62°, 25.36°, 26.59°, 30.96°, 36.75°, 52.07°, 54.71° and 66.53° can be identified as the diffractions from (210), (111), (020), (211), (301), (222), (040) and (123) planes of orthorhombic $Co_{16}S_{16}O_{96}$ (COD database code: 591-0314). In addition, it is observed that the diffraction peaks are very sharp, which suggests that the as-prepared nanosheets are composed of highly crystalline $Co_{16}S_{16}O_{96}$.

In order to further investigate the microstructure of the $Co_{16}S_{16}O_{96}$ nanosheets, extensive TEM analyses were carried out. Fig. 3a shows a low magnification TEM image of the as-fabricated

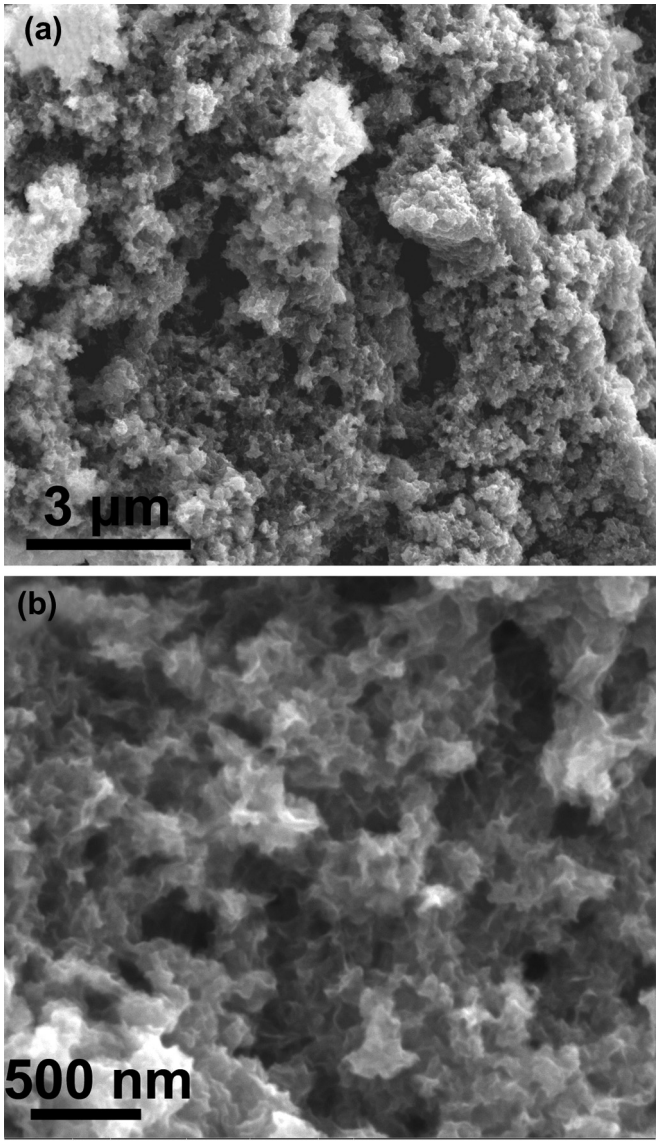

Fig. 1. SEM micrographs of the as-fabricated $Co_{16}S_{16}O_{96}$ nanosheets. (a) Overview and (b) zoomed view.

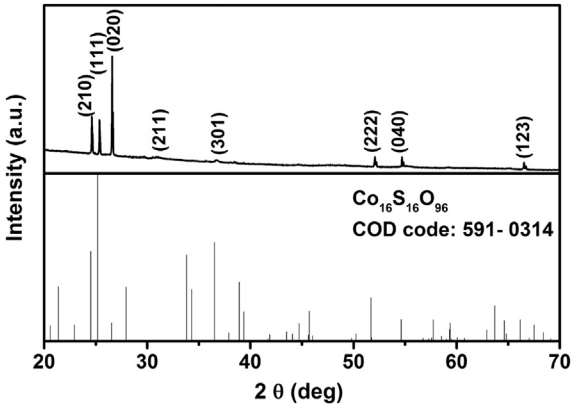

Fig. 2. XRD pattern of the as-prepared $Co_{16}S_{16}O_{96}$ nanosheets. For comparison, the standard powder diffraction pattern of $Co_{16}S_{16}O_{96}$ is also given (COD code: 591-0314).

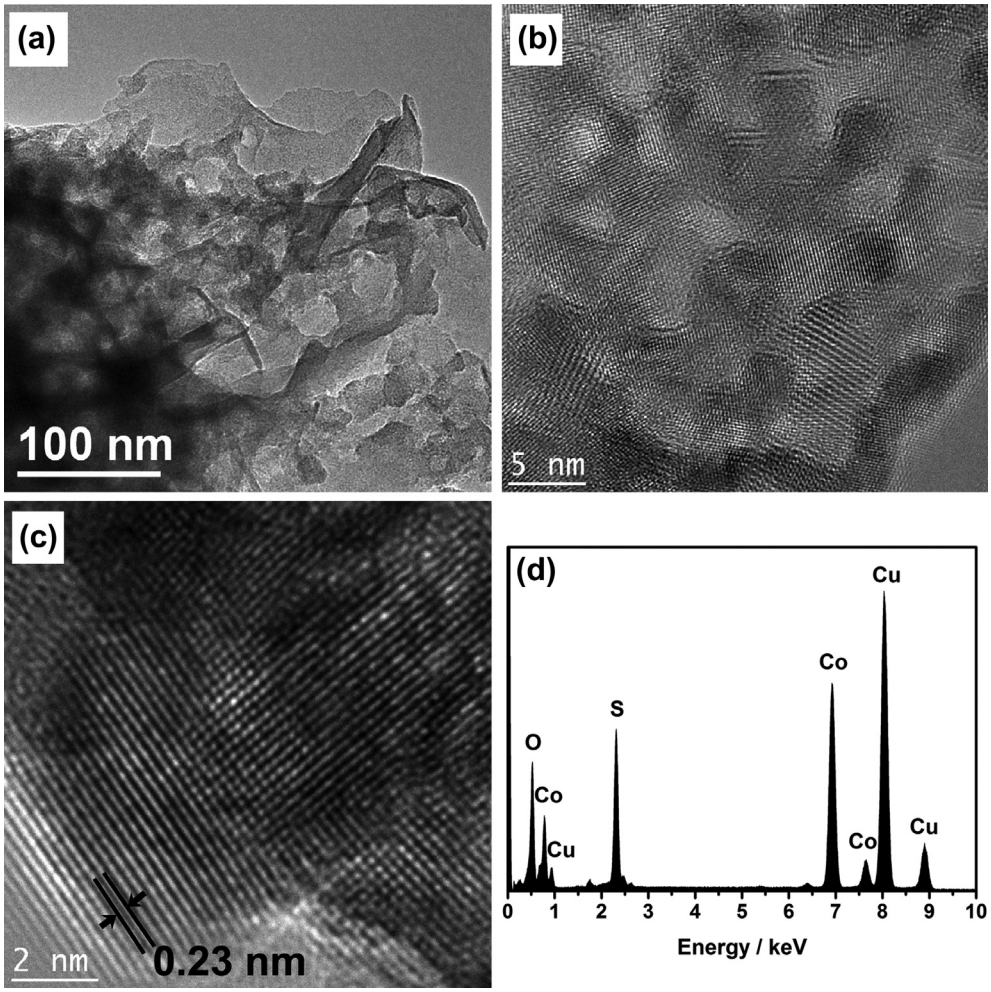

Fig. 3. TEM characterization of the as-fabricated $Co_{16}S_{16}O_{96}$ nanosheets. (a) A low-magnification TEM micrograph. (b) A high-magnification image showing the wavelike surface morphology and the mesoporous feature. (c) A representative HRTEM micrograph. (d) A typical EDX spectrum.

nanosheets from which one can clearly see the flexible sheet-like structure. It is noted that the nanosheets contain irregular pores with a pore size from a few to more than twenty nanometers. A close inspection in a typical nanosheet reveals that the nanosheet is highly crystalline, in consistence with the XRD result presented above; however, numerous defects and lattice distortions are observed which possibly result from the wavelike surface of the sheet and the presence of some tiny mesopores (Fig. 3b). Fig. 3c represents a high-resolution TEM micrograph taken from a single crystalline domain, in which the interplanar spacing of visible lattice fringes is 0.23 nm, corresponding to that of (211) planes of orthorhombic $Co_{16}S_{16}O_{96}$. Fig. 3d is a typical energy dispersive X-ray (EDX) spectrum of the nanosheets, which confirms that the nanosheets are composed of cobalt, sulfur and oxygen. The copper peaks are originated from the copper TEM grid.

Furthermore, the chemical state of the elements constituting the nanosheets was identified by XPS measurements. Fig. 4a shows a high-resolution XPS spectrum for O 1s. The main peak at the binding energy (BE) of 531.98 eV results from the binding of oxygen with sulfur, according to the previous study [14]; while the peak at 533.48 eV likely arises from the binding between cobalt and oxygen [15]. Fig. 4b reveals the S 2p lines of the spectrum. From the fitted curves, it is clearly seen that there are two peaks located at 168.78 eV and 169.98 eV, respectively, which are characteristic of sulfates/sulfites [14]. No peaks from sulfides are found in the spectrum, suggesting that cobalt does not directly bind with sulfur without the involvement of oxygen. The Co 2*p* XPS spectrum exhibits two main peaks at 782.08 eV and 797.78 eV, respectively, each with a satellite peak at a higher energy, as displayed in Fig. 4c. According to the literature [16], these two main peaks indicate the presence of Co^{2+} in the fabricated nanosheets.

The suitability of the as-fabricated $Co_{16}S_{16}O_{96}$ nanosheets as supercapacitor electrode materials was evaluated by cyclic voltammetry and galvanostatic charge/discharge tests. Fig. 5a shows typical CV curves of the $Co_{16}S_{16}O_{96}$ nanosheet electrode recorded at different scan rates in a 2 M KOH aqueous solution. In order to evaluate the contribution of the nickel foam current collector to the specific capacitance, a CV curve of bare nickel foam was also measured under the same conditions at a scan rate of 100 mV s^{-1} and presented in Fig. 5a. It is seen that compared with the nickel foam loaded with $Co_{16}S_{16}O_{96}$ nanosheets, the bare nickel foam only generates rather small specific current (in A g^{-1}) upon potential scan even at a high scan rate (i.e. 100 mV s^{-1}). This suggests that the contribution of nickel foam current collector to the specific capacitance can be neglected, which is in accordance with the observations reported before [7,12]. According to Fig. 5a, the shape of the cyclic voltammograms of the $Co_{16}S_{16}O_{96}$ electrode reveals a pseudocapacitive characteristic (i.e. redox peaks), different from

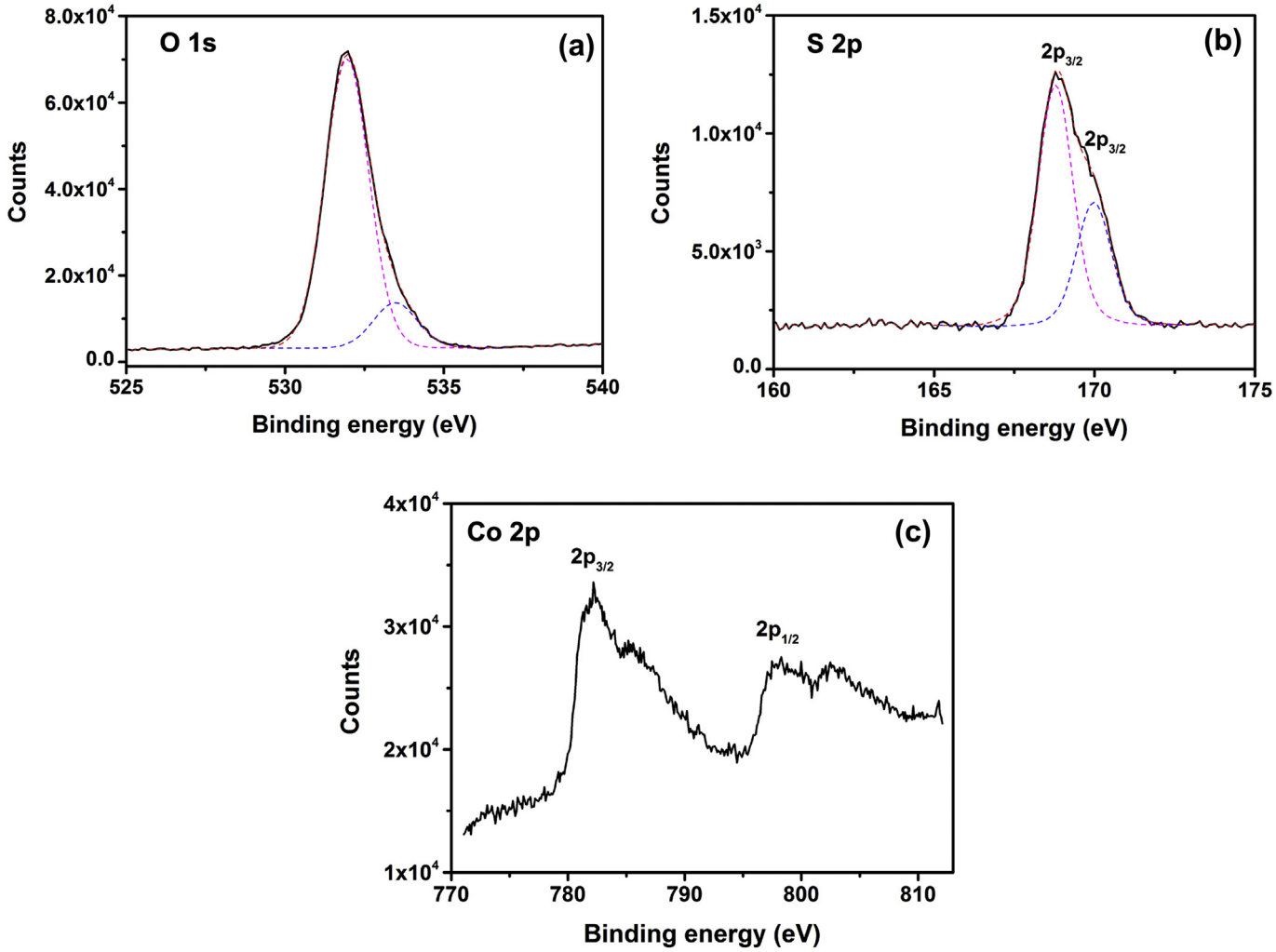

Fig. 4. X-ray photoelectron spectra (XPS) of the as-fabricated $Co_{16}S_{16}O_{96}$ nanosheets. (a) O 1s. (b) S 2p and (c) Co 2p. The dash lines denote the fitted curves of the measured XPS spectra.

the quasi-rectangular CV curves observed for EDLC capacitors [6]. As revealed in Fig. 4c, Co^{2+} ions are prevalent in the obtained $Co_{16}S_{16}O_{96}$ nanosheets. It is therefore assumed that the redox peaks could be associated with the quasi-reversible electron transfer process involving the Co^{2+}/Co^{3+} redox couple, similar as the case of CoS_2 reported before [12], because the redox potentials of these two compounds shown in CV curves are very close. However, the role of oxygen in the $Co_{16}S_{16}O_{96}$ nanosheets in the pseudocapacitive behavior remains unclear so far. Besides the cyclic voltammograms, the anodic peak current versus scan rates is also plotted in the inset of Fig. 5a, in which the linear relationship further corroborates the occurrence of surface redox reactions and the pseudocapacitive nature of the electrode.

Fig. 5b depicts the charge/discharge profiles of the $Co_{16}S_{16}O_{96}$ electrode recorded at different specific current densities in the potential range of $-0.05 - 0.4$ V vs. SCE. A shoulder peak can be clearly seen upon charge (at $\sim$0.3 V) and discharge (at $\sim$0.2 V), in good agreement with the redox potentials measured by CV. More importantly, it is found that the electrode was able to work over a broad range of current densities from 0.5 A g^{-1} to 50 A g^{-1}. The specific capacitance can be calculated to be 375, 351, 328, 293, 261, 228 and 170 F g^{-1} at 0.5, 1, 2, 5, 10, 20 and 50 A g^{-1}, respectively, which are much higher than that of carbon-based electrodes and even carbon nanotubes/MnO_2 hybrid electrodes reported before [17,18]. The specific capacitance and Coulombic efficiency (E) at different current densities versus cycle numbers are illustrated in Fig. 5c, which reveals that the $Co_{16}S_{16}O_{96}$ electrode has very good rate capability and can be efficiently discharged with an efficiency of >94.5%. In order to evaluate the cycling performance of the electrode, continuous charge/discharge tests were carried out at current densities of 1 A g^{-1} and 50 A g^{-1}, and the variation of specific capacitance as well as efficiency over cycle number is plotted in Fig. 5d. It is seen that at 1 A g^{-1}, the specific capacitance increases with the increasing cycle number, reaching 384 F g^{-1} and then remaining constant up to 4000 cycles. The increase in specific capacitance over cycle numbers, particularly at low rates, was also observed previously [19], and could be attributed to the increasing accessibility of electrochemically active sites upon cycling. It is also noteworthy that even at a current density as high as 50 A g^{-1}, the $Co_{16}S_{16}O_{96}$ electrode still exhibits specific capacitance of 170 F g^{-1}, and only loses 15.3% of the initial capacitance value after 4000 cycles, showing excellent cycling stability. Moreover, the Coulombic efficiency (E) of the electrode was found to be very high during the whole cycling tests (94.5% > E > 97.5% at 1 A g^{-1}, >99% at 50 A g^{-1}). This remarkable cycling performance is also confirmed by the fact that the shape of charge/discharge profiles at the beginning and at the end of the cycling tests nearly remains unchanged, as can be seen from Fig. 5e and f.

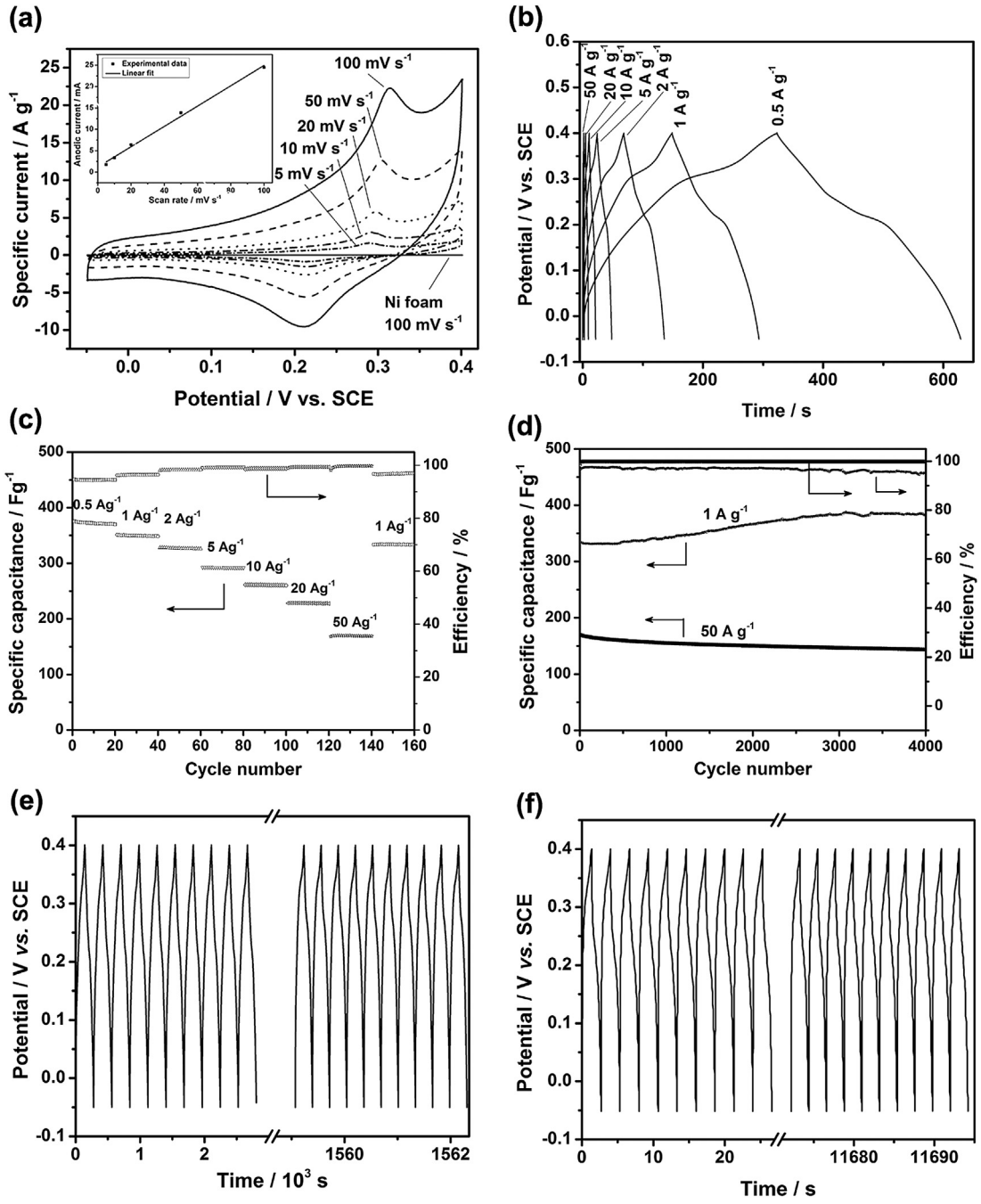

Fig. 5. Electrochemical performance of the $Co_{16}S_{16}O_{96}$ nanosheet electrode. (a) Cyclic voltammograms recorded at different scan rates. A cyclic voltammogram of bare nickel foam measured at 100 mV s^{-1} is also given for comparison. (b) Galvanostatic charge/discharge profiles at various specific current densities. (c) Rate capability of the electrode. (d) Cycling performance of the electrode at 1 A g^{-1} and 50 A g^{-1}. Charge/discharge profiles at the beginning and at the end of the cycling tests at a current density of (e) 1 A g^{-1} and (f) 50 A g^{-1}. Cycle numbers: 4000.

4. Conclusions

In summary, a new supercapacitive nanomaterial – $Co_{16}S_{16}O_{96}$ nanosheet has been synthesized by a facile hydrothermal method. These nanosheets are interconnected and exhibit porous sheet-like morphology. The supercapacitor electrode fabricated using the as-prepared $Co_{16}S_{16}O_{96}$ nanosheets reveals high specific capacitance, very good rate capability and excellent cycling stability, suggesting that these nanosheets hold great potential for use in high-performance supercapacitors.

Acknowledgments

The author thanks Dr. Cheuk Chi Albert NG for his help in XPS measurements.

References

[1] P. Simon, Y. Gogotsi, Nat. Mater. 7 (2008) 845.
[2] L.L. Zhang, X.S. Zhao, Chem. Soc. Rev. 38 (2009) 2520.
[3] G.A. Snook, P. Gao, A.S. Best, J. Power Sources 196 (2011) 1.

[4] W.T. Deng, X.B. Ji, Q.Y. Chen, C.E. Banks, RSC Adv. 1 (2011) 1171.
[5] M. Yang, J.X. Li, H.H. Li, L.W. Su, J.P. Wei, Z. Zhou, Phys. Chem. Chem. Phys. 14 (2012) 11048.
[6] M.K. Song, S. Cheng, H.Y. Chen, W.T. Qin, K.W. Nam, S.C. Xu, X.Q. Yang, A. Bongiorno, J. Lee, J.M. Bai, T.A. Tyson, J. Cho, M.L. Liu, Nano Lett. 12 (2012) 3483.
[7] G.W. Yang, C.L. Xu, H.L. Li, Chem. Commun. 48 (2008) 6537.
[8] P.K. Nayak, N. Munichandraiah, J. Electrochem. Soc. 155 (2008) A855.
[9] J.X. Li, M. Yang, J.P. Wei, Z. Zhou, Nanoscale 4 (2012) 4498.
[10] F. Tao, Y.Q. Zhao, G.Q. Zhang, H.L. Li, Electrochem. Commun. 9 (2007) 1282.
[11] Q.H. Wang, L.F. Jiao, H.M. Du, Y.C. Si, Y.J. Wang, H.T. Yuan, J. Mater. Chem. 22 (2012) 21387.
[12] L. Zhang, H.B. Wu, X.W. Lou, Chem. Commun. 48 (2012) 6912.
[13] T. Zhu, B.Y. Xia, L. Zhou, X.W. Lou, J. Mater. Chem. 22 (2012) 7851.
[14] I. Winter, C. Reese, J. Hormes, G. Heywang, F. Jonas, Chem. Phys. 194 (1995) 207.
[15] J. Yang, H.W. Liu, W.N. Martens, R.L. Frost, J. Phys. Chem. B 114 (2010) 111.
[16] P.A. Nikul'shin, A.V. Mozhaev, A.A. Pimerzin, N.N. Tomina, V.V. Konovalov, V.M. Kogan, Kinet. Catal. 52 (2011) 862.
[17] L.T. Le, M.H. Ervin, H.W. Qiu, B.E. Fuchs, W.Y. Lee, Electrochem. Commun. 13 (2011) 355.
[18] S.L. Chou, J.Z. Wang, S.Y. Chew, H.K. Liu, S.X. Dou, Electrochem. Commun. 10 (2008) 1724.
[19] Q.H. Wang, L.F. Jiao, H.M. Du, J.Q. Yang, Q.N. Huan, W.X. Peng, Y.C. Si, Y.J. Wang, H.T. Yuan, CrystEngComm 13 (2011) 6960.